

Enantioselective desymmetrization of meso-cyclopent-2-en-1,4-diacetate to 4-(R)-hydroxycyclopent-2-en-1-(S)-acetate using enzyme immobilized superparamagnetic nanocomposites

Maneea Eizadi Sharifabad^{1,2}, Ben Hodgson^{1,2} Mourad Jellite^{1,2} and Tapas Sen^{*1,2}

¹Centre for Materials Science, Chemistry Division, School of Forensic and Investigative Sciences

²Surface Patterning Group, Institute of Nanotechnology and Bio-engineering, University of Central Lancashire, Preston, United Kingdom, Email: MEizadi-sharifabad@uclan.ac.uk tsen@uclan.ac.uk

*Indicate the corresponding author

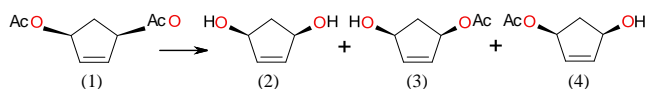
ABSTRACT

In this article, we report the method of fabrication of core-shell nanoparticles of superparamagnetic iron oxides core and amorphous / mesoporous silica shell along with hierarchically ordered porous silica containing embedded superparamagnetic iron oxide nanocomposites^{1,2}, surface engineering of such nanocomposites by novel Tri-phasic Reverse Emulsion (TPRE) method³ with aminopropyl triethoxy silane (APTS) followed by surface modification with glutaraldehyde for the immobilisation of *Candida Rugosa Lipase* (CRL) and *Pseudomonas Fluorescens Lipase* (PFL) via covalent coupling and used them as heterogeneous catalysts for the pharmaceutical important chiral catalysis “conversion of meso-cyclopent-2-en-1,4-diacetate to optically active products such as 4-(R)-hydroxycyclopent-2-en-1-(S)-acetate and 1-(R)-hydroxycyclopent-2-en-4-(S)-acetate”. It was found that CRL immobilised nanocomposites tend to produce both optical isomers with nearly 1:1 ratio whereas PFL immobilised nanocomposites produced only one optical isomer 4-(R)-hydroxycyclopent-2-en-1-(S)-acetate. The additional advantage of the solid supports was that they can be separated from the reaction mixture by simple one step magnetic separation and was suitable for storing at 4°C for used in several catalytic cycles without a significant loss of catalytic activity.

1 INTRODUCTION

Enzymes are well known as catalysts for various bio-transformations however, removal of such expensive enzymes from the reaction mixtures can be very difficult and costly. Hence, immobilization of enzymes on solid support is a very important step for the recovery and recycling of the enzymes after the catalysis reactions. Magnetisable solid support could have an additional benefit as they can be separated from the reaction mixture by the influence of an external magnetic field. In this context, superparamagnetic nanocomposites and nanoparticles have been previously used by our group to immobilize lipases for ester hydrolysis.^{1,2,4} The use of immobilized enzymes is

particularly important as they exhibit increased stability and catalytic activity compared with free enzymes.^{5,6} Bio-transformations catalysed by immobilised enzymes or microbial cells have tremendous potential in the industrial production of fine chemicals.^{7,8} For example, in the pharmaceutical industry enantiomerically pure 4-(R)-hydroxycyclopent-2-en-1-(S)-acetate (see product 3 in the reaction scheme 1) or its enantiomer 1-(R)-hydroxycyclopent-2-en-4-(S)-acetate (see product 4 in the reaction scheme 1) are starting materials for the synthesis of prostaglandins^{9,10} prostacyclins and thromboxanes¹¹. These starting materials can be synthesized bio-catalytically either (a) by the enzymatic hydrolysis of the diacetate (1 in the reaction scheme) or (b) transesterification of diol (2, see reaction scheme 1) using lipases. Considering the large market demand for high cost chiral intermediates, like 3 and 4 in the reaction scheme 1, development of economically viable enzymatic technology for their large-scale preparation represents an important synthetic objective. Herein, we report a systematic study of the immobilization of two different enzymes (CRL and PFL) onto two solid supports (i.e. HOPMN and core-shell SPIONs) for the enzymatic hydrolysis of reactant 1 (see reaction scheme 1). The materials were initially tested for model catalysis (hydrolysis of p-nitro phenyl palmitate to p-nitrophenol and palmitic acid) in order to standardise the best catalytic supports for the chiral catalysis reaction (see reaction scheme 1).



Reaction Scheme 1 Enzymatic hydrolysis of meso-cyclopent-2-en-1,4-diacetate

2 EXPERIMENTAL

2.1 Synthesis of Magnetite Cores

Bare superparamagnetic iron oxide nanoparticles (SPIONs) were synthesized following Massart method¹² by co-

precipitation of an aqueous solution of ferrous and ferric chloride in the presence of ammonium hydroxide with a slight modification from our earlier reported protocol.¹³

2.2 Synthesis of Core-Shell Silica-Magnetite Nanoparticles

Mesoporous silica coated superparamagnetic iron oxide nanoparticles were prepared by coating the ultrasmall magnetite nanoparticles prepared from section 2.1. The coating was carried out using tetraethoxy silane (TEOS) as a silica source, cetyl trimethyl ammonium bromide (CTAB) as surfactant under alkaline conditions (NH_4OH as a base) at 25°C under stirring for overnight. The materials were washed several times with acidic ethanolic solution followed by de-ionized water to remove the template hence to fabricate the mesoporous silica shell.

2.3 Synthesis of superparamagnetic iron oxide embedded hierarchically ordered porous silica

The novel hierarchically ordered porous silica with embedded superparamagnetic iron oxide nanoparticles were synthesised using the previously published protocol by our group^{1,2} using a multiple templating route such as monodispersed polystyrene latex spheres and tri-block copolymer F127 as the templates. Tetraethyl orthosilica and ferrous and ferric chlorides were used as the source of silica and iron in order to fabricate the novel materials.

2.4 Surface engineering of superparamagnetic core-shell and hierarchically ordered porous silica nanocomposites

Surface activation of nanoparticles was performed using TPPE method.³ 150 mg of nanocomposites separated from the aqueous solution by magnetic separation and were dispersed in 30ml of toluene in the presence of 5g of Triton X100 as a surfactant. APTS was added to the suspension to a final concentration of 2% w/v and the mixtures were kept on rotator at 40 rpm for 24 hours inside an incubator previously set at 50°C . After 24 hours the nanoparticles were collected by magnetic separation and washed 3 times with coupling solution (0.8% vol to vol of glacial acetic acid in methanol). The surface amine densities of various materials were measured by standard colorimetric assay^{14,15} using an UV sensitive molecule, 4-nitrobenzaldehyde by measuring the optical density at 280nm.

Conversion of surface amine groups to aldehyde groups was performed by using glutaraldehyde in SSC buffer ($20\times$) for 3 hours incubation at 18°C with end-over-end rotation (40 rpm). After 3 hours, the nanocomposites were washed

($3\times$ with 5 mL of $1\times$ SSC buffer followed by $3\times$ with 5 mL of PBS buffer)¹⁵ via magnetic separation.

2.5 Immobilization of CRL and PFL enzymes on the surface aldehyde groups modified nanocomposites

50 mg of the nanocomposites were added to a 4 ml of lipase solution (concentration of 1 mg/ml lipase in phosphate buffer). The mixture was incubated at 18°C with constant rotation at 40 rpm for 20 h. After the incubation period, the nanocomposites were separated and the quantitative estimation of surface attached enzymes was calculated by determining the amount of enzymes left in the supernatant by measuring the absorption at $\lambda_{595\text{nm}}$ using UV/Vis spectrophotometry following the well established Bradford Essay¹⁶. Figure 1 presents a schematic diagram of surface functionalisation and enzyme immobilisation to the superparamagnetic nanocomposites *via* covalent coupling.

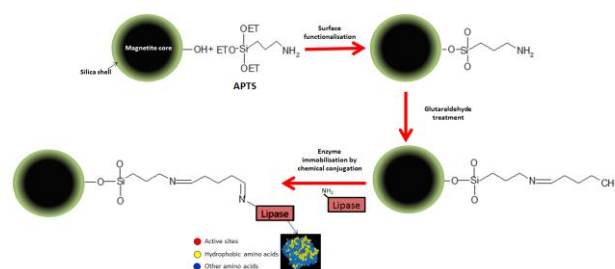


Figure 1: Surface functionalization of superparamagnetic nanocomposites and the immobilization of enzymes to the surface *via* covalent bonding

2.6 Model catalysis (hydrolysis of p-nitrophenyl palmitate) and the enzymatic hydrolysis of *meso*-cyclopent-2-en-1,4-diacetate

The model catalysis reaction (hydrolysis 4-nitro phenyl palmitate) was carried out using 15mg lipase immobilized nanocomposites reacting with 1mL of 4-nitro phenyl palmitate solution ($3.74\ \mu\text{mol ml}^{-1}$) prepared in a 1:1 mixture of isopropanol and reagent A (0.0667g Gum Arabic + 12mL of 250mM Tris-HCl buffer, pH 7.8 + 48mL of deionized water + 0.267g of sodium deoxycholate) at 20°C for 4 hrs in 1.5mL Eppendorf tube by end-over-end rotation. The reaction product, 4-nitrophenol was measured by measuring the absorbance at $\lambda_{410\text{nm}}$ following a reported protocol.^{2,17}

Enzymatic hydrolysis: 50 μmol of *meso*-cyclopent-2-en-1,4-diacetate was added into a solvent mixture (hexane : water :: 8:2). 500 μg of free or equivalent amount of lipases immobilised on nanocomposites were then added into the reaction mixture and was incubated at 25°C with

end-over-end rotation (40 rpm) for 48 hours. During the reaction, a 5 μL aliquot from the water layer (as the products are soluble in water but not in hexane) was withdrawn at different time intervals (1 h, 4 h, 24 h and 48 h) and analyzed by GC and GCMS using a chiral column. The hexane layer was used to monitor the concentration of reactant as the reactant is mostly soluble in hexane and sparingly soluble in water. Gas chromatography (GC) analysis was carried out on a Varian Chrompack CP-3380 Gas Chromatograph (California, USA) using nitrogen as the carrier gas and a chiral column; Supelco BETA DEXTM 110 fused silica capillary column (length = 30 m, internal diameter = 0.25 mm, film thickness 0.25 μm). The GC condition was as follows: start at 50°C with a ramp of 10°C per minute and stop at 200°C.

All materials were characterised by powder X-ray diffraction, Scanning Electron Microscopy (SEM), Transmission Electron Microscopy (TEM) and Surface area measurement by BET method using nitrogen gas adsorption.

3 RESULTS AND DISCUSSION

Figure 2 presents the electron micrographs of core shell and hierarchically ordered porous nanocomposites.

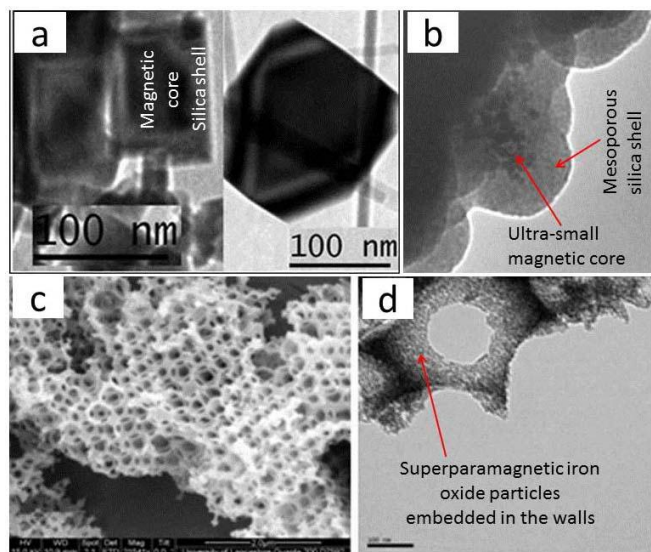


Figure 2: TEM images of core-shell nanoparticles of rhombic magnetic core and amorphous silica shell (a), ultra-small superparamagnetic iron oxide core and mesoporous silica shell (b), hierarchically ordered porous silica nanocomposites with embedded superparamagnetic iron oxides nanoparticles (d) and SEM image of hierarchically ordered porous silica nanocomposites with embedded superparamagnetic iron oxides nanoparticles.

The core shell nanocomposites were formed with superparamagnetic iron oxides cores of both spherical and

rhombic morphology which were coated with either amorphous or mesoporous silica shells (see Fig. 2a and 2b). The hierarchically ordered porous nanocomposites (see Fig. 2c and 2d) possessed macro-meso and microporosity with interconnecting pores and embedded superparamagnetic iron oxide nanoparticles (Fig.2d) into the walls of the silica matrix.

The nanoparticles were different in sizes from 100nm (rhombic core-shell) to 300nm (spherical core-shell). The hierarchically ordered porous nanocomposites were observed to be formed with macropores of diameter from 100nm to 500nm with the disordered mesoporous walls of mesopore diameter of around 10nm containing embedded superparamagnetic iron oxide particles of sizes of around 10nm. The superparamagnetic core materials were characterised as magnetite from powder XRD (data not shown). The surface areas of the rhombic core-shell nanoparticles were measured to be around 20m²/g, spherical core-shell nanoparticles was around 1100m²/g and the hierarchically ordered porous nanocomposites was around 200m²/g. Variable sample magnetometer (VSM) data indicated that all materials were superparamagnetic in nature with zero magnetic remanence (M_R) and the saturation magnetisation values were 13 emu/g (hierarchically ordered porous silica), 15 emu/g (spherical core-shell nanoparticles) and around 70 emu/g (rhombic core-shell nanoparticles) respectively.

All materials exhibited catalytic conversion of p-nitrophenyl palmitate to p-nitrophenol and palmitic acid in the order of 1×10^3 to 2.5×10^3 μmol of p-nitrophenyl palmitate per g of enzymes as a model catalysis reaction.

Figure 3 presents the formation of pharmaceutically important optical isomer 4-(R)-hydroxycyclopent-2-en-1-(S)-acetate as a product from the enzymatic hydrolysis of meso-cyclopent-2-en-1,4-diacetate using free CRL, PFL and chemically and physically immobilised CRL and PFL onto the spherical core-shell nanocomposites.

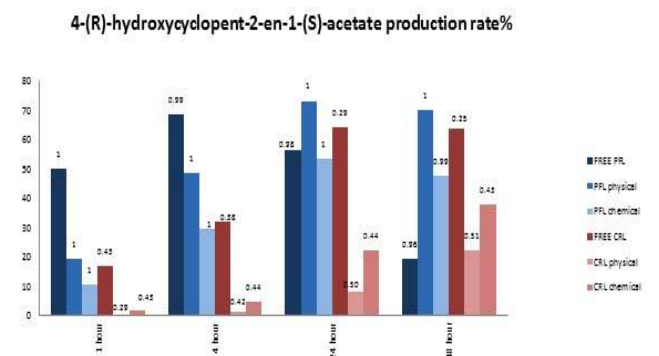


Figure 3: Formation of 4-(R)-hydroxycyclopent-2-en-1-(S)-acetate by the enzymatic hydrolysis of meso-cyclopent-2-en-1,4-diacetate using free and immobilised CRL and PFL.

Free PFL performed better than free CRL. The immobilised PFL by covalent bonding i.e. chemically attached (see figure 1) and physically adsorbed performed in a similar way to the free PFL after 24 hrs of reaction. However, when the supported materials were reused, physically adsorbed enzyme immobilised support performed relatively less conversion during the 2nd and 3rd cycles and this may be due to the leaching of enzymes into the solution during the first cycle of catalytic reaction. The chemically attached enzymes onto the support retained their catalytic activity up to 3 cycles indicating the importance of surface modification and immobilisation via chemical bonding based on figure 2. CRL materials exhibited lower % conversion of the reactant compared to PFL immobilised materials. The major difference between CRL and PFL materials was the relative ratio of two optical isomers (3 and 4) by enzymatic hydrolysis of reactant 1 (see reaction scheme 1). Free CRL and CRL immobilised nanocomposites produced both optical isomers (3 and 4 in the reaction scheme 1) with nearly 1:1 ratio whereas the PFL immobilised materials produced only optical isomer (3 in the reaction scheme 1). The total conversion of reactant 1 for free PFL was higher but the majority of the product was unwanted diol (product 2 in the reaction scheme 1).

4 CONCLUSIONS

In conclusion, a range of superparamagnetic nanocomposites were used as an important solid support for the immobilisation of two different enzymes (CRL and PFL). PFL immobilised materials produced a higher yield with enantiomerically pure product 4-(R)-hydroxycyclopent-2-en-1-(S)-acetate whereas CRL immobilised materials produced lower yield compared to PFL immobilised materials with a mixture of two optical isomers 4-(R)-hydroxycyclopent-2-en-1-(S)-acetate and 1-(R)-hydroxycyclopent-2-en-4-(S)-acetate. Free PFL was efficient in the conversion of the reactant (1) but produced mostly unwanted product diol form (2). This is an important work for the production of chiral chemicals of pharmaceutical interest using enzyme immobilised magnetisable solid support (superparamagnetic nanocomposites).

5 ACKNOWLEDGEMENTS

Authors thank to Royal Society for two small research grants (2011-12 and 2012-13) to carry out this work. Ben Hodgson and Maneea Eizadi thank to the University of Central Lancashire for partial funding to carry out their PhD studies. Ben Hodgson also thank to Q-bioanalytic GmbH, Germany for the partial funding during the 2nd and 3rd year of his PhD studies.

REFERENCES

1. Sen, T. *NSTI-Nanotech* 2010, CRC Press, Taylor & Francis Group: **2010**; pp 784-787.
2. Sen, T., I.J. Bruce, and T. Mercer, *Chem. Commun.*, 2010, **46**(36): p. 6807.
3. Sen, T.; Bruce, I. J. *Scientific Reports*, 2012, **2**: 564 | DOI: 10.1038/srep00564 (Nature publishing Group)
4. Dyal, A.; Loos, K.; Noto, M.; Chang, S. W.; Spagnoli, C.; Shafi, K. V. P. M.; Ulman, A.; Cowman, M.; Gross, R. A. *J. Am. Chem. Soc.* **2003**, *125*, 1684.
5. Wong, L. S.; Okrasa, K.; Micklefield, J. *Org. Biomol. Chem.* **2010**, *8*, 782.
6. Yang, Z.; Si, S.; Zhang, C. *Biochem. Biophys. Res. Commun.* **2008**, *367*, 169.
7. Balcao, V.M.; Paiva, A.L.; Malcata, F.X. *Enzyme. Microb. Technol.* **1996**, *18*, 392.
8. Klivanov, A.M. *Science* **1982**, *219*, 722
9. Noyori, R.; Suzuki, M. *Angew. Chem. Int. Ed.* **1984**, *23*, 847.
10. Danishefsky, S.J.; Cabal, M.P.; Choe, K. *J. Am. Chem. Soc.* **1989**, *111*, 3456.
11. Ghorpade, S.R.; Kharul, R.K.; Joshi, R.R.; Kalkote, U.R.; Ravindranathan, T. *Tetrahedron. Asymm.* **1999**, *10*, 891.
12. Massart, R., et al., *J. Magn. Magn. Mater.*, 1995, **149**(1-2): p. 1-5.
13. Sen, T.; Magdassi, S.; Nizri, G.; Bruce, I. J. *Micro & Nano Lett.* **2006**, *1*, 39.
14. Moon, J. H.; Kim, J. H.; Kim, K.; Kang, T. H.; Kim, B.; Kim, C. H.; Hahn, J. H.; Park, J. W. *Langmuir* **1997**, *13*, 4305-4310.
15. Sen, T.; Bruce, I. J.; *Langmuir* **2005**, *21*, 7029-7035.
16. M. Bradford, *Anal. Biochem.* **1976**, *72*, 248-254.
17. Gupta, N.; Rathi, P.; Gupta, R. *Anal. Biochem.* **2002**, *311*, 98-99.